

100-K Superconducting Phases in the Tl-Ca-Ba-Cu-O System

R. M. Hazen, L. W. Finger, R. J. Angel, C. T. Prewitt, N. L. Ross, and C. G. Hadidiacos
Geophysical Laboratory, Carnegie Institution of Washington, Washington, D.C. 20008

P. J. Heaney and D. R. Veblen
Department of Earth and Planetary Sciences, The Johns Hopkins University, Baltimore, Maryland 21218

and

Z. Z. Sheng, A. El Ali, and A. M. Hermann
Department of Physics, University of Arkansas, Fayetteville, Arkansas 72701
 (Received 22 February 1988)

Two superconducting phases, $\text{Tl}_2\text{Ca}_2\text{Ba}_2\text{Cu}_3\text{O}_{10+\delta}$ (2223) and $\text{Tl}_2\text{Ca}_1\text{Ba}_2\text{Cu}_2\text{O}_{8+\delta}$ (2122), both with onset T_c near 120 K and zero resistivity at 100 K, have been isolated from samples in the Tl-Ca-Ba-Cu-O system. The new 2223 superconductor has a $5.40 \times 5.40 \times 36.25$ -Å³ pseudotetragonal unit cell. The 2122 superconductor, which appears to be structurally related to $\text{Bi}_2\text{CaSr}_2\text{Cu}_2\text{O}_{8+\delta}$, has a $5.44 \times 5.44 \times 29.55$ -Å³ pseudotetragonal subcell. The 2223 phase is probably related to 2122 by the addition of extra calcium and copper layers.

PACS numbers: 74.70.Vy

High-temperature superconductivity in oxides, first reported in the K_2NiF_4 ¹ and $\text{YBa}_2\text{Cu}_3\text{O}_7$ ² structures, has recently been observed in new systems containing copper, alkaline earths, and bismuth³⁻⁵ or thallium.⁶⁻⁸ The bismuth-bearing superconductor phase has been identified as $\text{Bi}_2\text{Ca}_1\text{Sr}_2\text{Cu}_2\text{O}_{8+\delta}$.⁹ That phase, the third known high- T_c structure, possesses a novel layered atomic arrangement with alternating bismuth-oxide double layers and pairs of $[\text{CuO}_2]_\infty$ layers separated by calcium.¹⁰⁻¹²

In this Letter we describe phases that occur in 100-K superconducting samples synthesized by Sheng and Hermann in the Tl-Ca-Ba-Cu-O (TCBCO) system.⁸ We have isolated two new high- T_c oxide phases, both of which bear a close structural relationship to the bismuth superconducting compound.

We studied three superconducting TCBCO samples, designated TCBCO-1, TCBCO-2, and TCBCO-3. Initial Tl:Ca:Ba:Cu metal ratios for these samples are 2:2:1:3, 2:3:1:3, and 2:2:2:3, respectively. (Our studies of samples in the Tl-Ba-Cu-O system,^{6,7} which contains a different superconducting phase with zero resistivity at approximately 80 K, are in progress.) A typical procedure for the synthesis of TCBCO samples is as follows. Appropriate amounts of Tl_2O_3 , CaO, and BaCu_3O_4 (or $\text{Ba}_2\text{Cu}_3\text{O}_5$) were completely mixed, ground, and pressed into a pellet. A quartz boat containing the pellet was then put into a tube furnace, which had been preheated to 880–910 °C. The sample was heated for 3 to 5 min in flowing oxygen and furnace cooled to room temperature in 1 to 1.5 h. The barium cuprate starting materials were prepared according to the procedure of Hermann and Sheng.¹³

The thallium-bearing material displays an onset temperature of 120 K, a midpoint T_c near 110 K, and zero

resistivity above 100 K. Figure 1 shows the four-probe resistance-temperature variation for TCBCO-1 and TCBCO-3 samples. In the former case zero resistance is reached at 106 K, in the latter at 102 K. The zero-resistance points represent values of resistivity less than 10^{-6} Ω cm. The superconducting behavior of TCBCO samples is sensitive to preparation conditions.^{7,8}

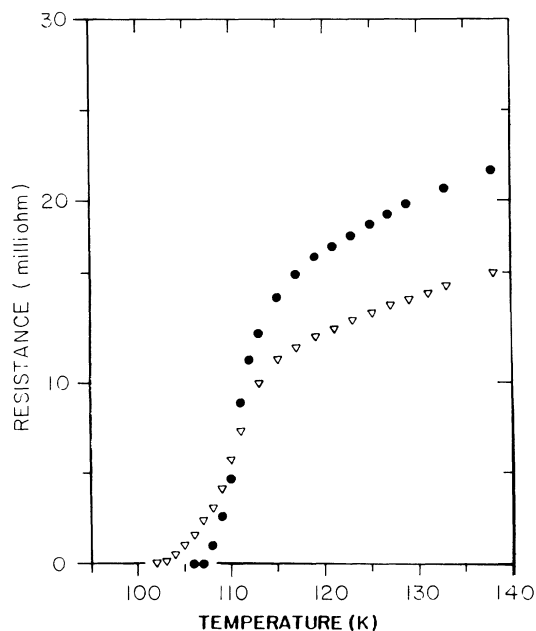


FIG. 1. Resistance-temperature measurements for two TCBCO samples. Circles denote data on a 2213 composition (TCBCO-1) and the triangles indicate a 2223 sample (TCBCO-3).

TABLE I. Powder x-ray diffraction lines for the high- T_c phase $Tl_2Ca_1Ba_2Cu_2O_{8+\delta}$ (2122). Patterns were obtained with filtered Cu radiation.

H	K	L	D_{obs}	D_{calc}	I/I_0
0	0	2	14.7	14.8	5
0	0	6	4.85	4.94	5
0	0	10	2.95	2.96	9
1	0	9	2.82	2.81	87
2	0	0	2.71	2.72	100
1	1	8	2.663	2.665	14
1	1	9	2.508	2.498	5
2	0	5	2.475	2.471	5
2	1	0	2.433	2.433	17
2	1	2	2.395	2.401	10
2	1	4	2.315	2.311	8
2	2	0	1.926	1.924	47
3	0	0	1.814	1.814	18
3	1	6	1.623	1.624	14
3	0	9	1.588	1.588	21
1	0	18	1.573	1.573	5
1	1	18	1.511	1.511	10
4	0	0	1.360	1.360	12
2	1	21	1.218	1.219	13

X-ray powder diffraction patterns of the TCBCO samples differed from those of previously described superconducting phases. Samples were examined by optical and electron microscopy, x-ray powder diffraction, and electron microanalysis. Electron microanalyses were obtained on a JSM model 35 scanning electron microscope, operated at 20 kV and 0.01- μ A beam current with a 2.5- μ m spot size. Standards include pure Tl and Cu metal, Ba-bearing glass, and a diopside₆₅-jadeite₃₅ pyroxene glass. We employed a Philips model EM420 transmission electron microscope (TEM) with EDAX Si-Li detector and a Princeton Gamma-Tech model 4 data analysis system. TEM samples were mounted on holey-carbon, Be-mesh grids to avoid Cu contamination during qualitative analysis.

Sample TCBCO-1 consists of two principal phases, both of which are black, opaque, and fine grained with particle sizes less than 10 μ m maximum diameter. Electron microprobe analysis of more than 30 grains revealed two distinct, nearly stoichiometric compounds. Approximately 80% of the sample has metal ratios of 2:2:2:3 yielding a formula $Tl_2Ca_2Ba_2Cu_3O_{10+\delta}$ while 20% has approximate ratios 1:4:0:5 corresponding to $(Tl_{0.19}Ca_{0.81})CuO_{2+\delta}$. Electron diffraction of this barium-poor compound reveals a large orthorhombic unit cell approximately $5.4 \times 17.4 \times 43.4 \text{ \AA}^3$, with a prominent pseudocubic subcell, approximately 5.4 \AA on edge. The material is highly twinned and displays streaking parallel to the long axis. Two additional samples with the 2223 and 1405 stoichiometries as starting compositions were synthesized. The 1405 compound is a semiconductor; 2223 is a high- T_c superconductor.

Sample TCBCO-2 contains both the 2223 and 1405 phases, which comprise approximately 70% and 5% of the sample, respectively. The composition of 2223 from this sample is more variable than in TCBCO-1. The sum of Ca + Ba is always close to 4, but the ratio of these elements varies from 50:50 to 45:55. Two additional phases, observed during electron microanalysis, have nearly stoichiometric metal ratios of 2:1:2:2 and 3:4:0:0. These compounds each comprise approximately 15% of the sample. The 2122 phase, corresponding to $Tl_2Ca_1Ba_2Cu_2O_{8+\delta}$, is of special interest because of its apparent similarity to the 90-K superconducting phase $Bi_2Ca_1Sr_2Cu_2O_{8+\delta}$.⁹⁻¹¹ Several electron microanalyses of material that appears to be single phase yielded compositions intermediate between 2122 and 2223. It is likely that intergrowths of these two compounds occur on a very fine scale and further TEM studies are in progress.

Sample TCBCO-3, with a starting metal stoichiometry of 2:2:2:3, consists primarily of the 2122 phases plus unreacted oxides of copper and calcium. None of the 2223 phase was detected; we conclude therefore, that 2122 is also a high- T_c superconductor. This 2122 phase has pseudotetragonal unit-cell dimensions of 5.44×5.44

TABLE II. Powder x-ray diffraction lines for the high- T_c phase $Tl_2Ca_2Ba_2Cu_3O_{10+\delta}$ (2223). Pure silicon (National Bureau of Standards Standard Reference Material 640) was used as an internal standard. Patterns were obtained with filtered Cu radiation.

h	k	l	d_{obs}	d_{calc}	I/I_0
0	0	2	17.8	18.1	25
0	0	4	8.93	9.06	1
0	0	6	5.95	6.04	1
0	0	8	4.46	4.52	10
1	1	5	3.39	3.38	39
1	0	9	3.228	3.228	15
1	1	7	3.079	3.073	87
0	0	12	3.028	3.021	1
1	1	9	2.766	2.771	100
2	0	0	2.696	2.699	63
2	0	2	2.663	2.669	15
2	0	5	2.522	2.529	41
1	0	13	2.481	2.478	19
2	1	1	2.408	2.409	6
2	0	8	2.321	2.319	15
2	0	10	2.166	2.165	7
1	0	16	2.090	2.089	16
1	1	17	1.862	1.862	26
0	0	21	1.726	1.726	22
3	1	7	1.622	1.621	15
2	0	19	1.557	1.558	15
2	2	14	1.537	1.536	22
2	2	16	1.459	1.460	11
3	2	7	1.439	1.438	11
0	0	26	1.394	1.394	11
4	1	7	1.269	1.269	15

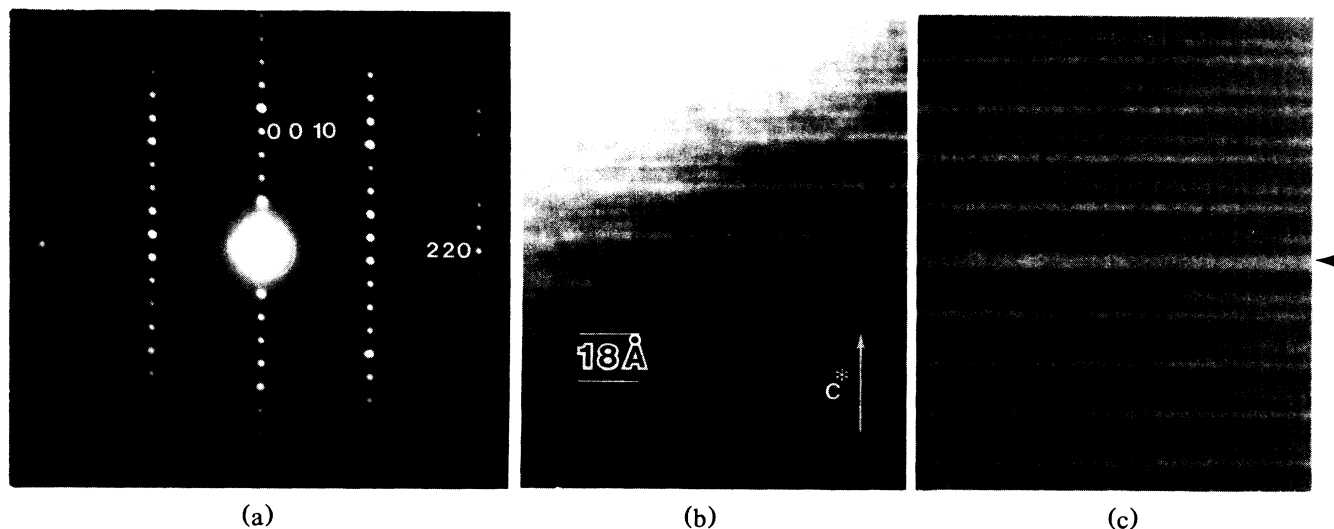


FIG. 2. (a) $[1\bar{1}0]$ Selected-area electron diffraction pattern of 2223 superconductor. (b) The corresponding lattice image reveals a prominent 18-Å layering parallel to (001), similar to that of the bismuth 2122 superconductor (Refs. 9 and 14). (c) Defects in the layering (arrow) are relatively uncommon in the 2223 phase compared to the structurally related bismuth 2122 superconductor.

$\times 29.5 \text{ \AA}^3$, based on x-ray powder diffraction of samples TCBCO-2 and TCBCO-3. The positions and intensities of powder lines (Table I) confirm that this superconductor has a structure that is similar to, but in detail different from, that of $\text{Bi}_2\text{Ca}_1\text{Sr}_2\text{Cu}_2\text{O}_{8+\delta}$, which has an orthorhombic unit subcell $5.41 \times 5.44 \times 30.78 \text{ \AA}^3$. Both phases display a prominent and diagnostic (002) powder line corresponding to $a \approx 15 \text{ \AA}$ ($2\theta \approx 6^\circ$ with Cu radiation). This spacing in bismuth 2122 is 15.4 \AA , compared with 14.8 \AA for the thallium 2122 phase. Transmission-electron-microscopy investigation of the thallium 2122 phase is now in progress.

Electron and x-ray diffraction studies of the 2223 phase reveal a well-ordered tetragonal or pseudotetragonal unit cell with $a = 5.399 \pm 0.002 \text{ \AA}$ and $c = 36.25 \pm 0.02 \text{ \AA}$. Table II lists positions and intensities of 26 powder lines. The presence of a strong 18-Å (002) powder line ($2\theta \approx 5^\circ$ with Cu radiation) is a diagnostic feature. Electron diffraction patterns of 2223 from sample TCBCO-1 (Fig. 2) show little of the streaking or other irregularities associated with the bismuth 2122 superconductor.¹¹ High-resolution images of c^* reveal a distinct layered structure, similar to that of the 2122 phase,¹⁴ but with few stacking faults. No superlattice reflections are observed, but faint ringlike diffraction around several diffraction maxima (Fig. 3) may indicate short-range ordering of defects.¹⁵

We conclude from compositional, powder x-ray, and TEM data that the bismuth 2122 and thallium 2122 and 2223 are closely related structures. The $\text{Bi}_2\text{CaSr}_2\text{Cu}_2\text{O}_{8+\delta}$ and presumably the $\text{Tl}_2\text{CaBa}_2\text{Cu}_2\text{O}_{8+\delta}$ 2122 structures have a 15-Å layer repeat of bismuth or thallium oxide double layers and pairs of copper-oxygen planes separated by calcium. The 2223 structure of $\text{Tl}_2\text{Ca}_2\text{Sr}_2\text{Cu}_2\text{O}_{10+\delta}$

has a slightly longer 18-Å repeat and an extra copper and calcium per formula unit. We suggest that the structure of 2223 is similar to that of 2122 but with three copper-oxygen planes separated by calcium. Thus all four known high- T_c structure types possess $[\text{CuO}_2]_\infty$ planes. Confirmation and detailed analysis of this structure must await the availability of purer powder samples or larger single crystals.

In spite of the many similarities, the bismuth and thallium superconductors appear to differ in one important respect. The bismuth phase displays a pronounced lay-



FIG. 3. Selected-area diffraction pattern of the 2223 phase reveals faint ringlike diffraction effects that surround some diffraction maxima. This pattern, which is consistent with the $[21\bar{1}]$ zone axis, may result from point-defect clusters or other short-range ordering (Ref. 15).

ered morphology typical of layer silicates. The thallium phases, on the other hand, have no obvious perfect cleavages when observed by electron microscopy. This difference in morphology could be the result of a high density of stacking faults in the bismuth phase. More likely, however, the shorter *c*-axis spacing and more ordered appearance of the thallium 2122 material seems to imply a corresponding difference in interlayer bonding of the bismuth and thallium compounds.

Work done at the Geophysical Laboratory is supported by National Science Foundation Grants No. EAR8419982, No. EAR8608941, and No. EAR8618649 and the Carnegie Institution of Washington. Work done at The Johns Hopkins University is supported by National Science Foundation Grant No. EAR8609277.

Note added.—The 80-K superconducting phase in the Tl-Ba-Cu-O (calcium absent) system has been identified by electron microprobe analysis and powder x-ray diffraction to have the approximate composition $\text{Tl}_2\text{Ba}_2\text{CuO}_{6+\delta}$ and a tetragonal or pseudotetragonal unit cell approximately $5.4 \times 5.4 \times 23.5 \text{ \AA}^3$. This phase, which we designate 2021, has a copper-oxygen monolayer, as compared with the bilayer and trilayer features of 2122 and 2223. These homologous phases are members of the structural series $\text{Tl}_2\text{Ca}_{N-1}\text{Ba}_2\text{Cu}_N\text{O}_{2N+4+\delta}$, where *N* corresponds to the number of adjacent copper-oxygen layers. The increase in observed T_c with *N* may be related to an increase in the density of states; it is predicted, therefore, that related structures with more than three Cu-O layers (e.g., $\text{Tl}_2\text{Ca}_3\text{Ba}_2\text{Cu}_4\text{O}_{12+\delta}$ or 2324) will display higher T_c .

¹J. G. Bednorz and K. A. Müller, *Z. Phys. B* **64**, 189 (1986).

²M. K. Wu, J. R. Ashburn, C. J. Torng, P. H. Hor, R. L. Meng, L. Gao, Z. J. Huang, Y. Q. Wang, and C. W. Chu, *Phys. Rev. Lett.* **58**, 908 (1987).

³C. Michel, M. Hervieu, M. M. Borel, A. Grandin, F. Deslandes, J. Provost, and B. Raveau, *Z. Phys. B* **68**, 421 (1987).

⁴H. Maeda, Y. Tanaka, M. Fukutomi, and T. Asano, *Jpn. J. Appl. Phys. Lett.* (to be published).

⁵C. W. Chu, J. Bechtold, L. Gao, P. H. Hor, Z. J. Huang, R. L. Meng, Y. Y. Sun, Y. Q. Wang, and Y. Y. Xue, *Phys. Rev. Lett.* **60**, 941 (1988).

⁶Z. Z. Sheng, A. M. Hermann, A. El Ali, C. Almason, J. Estrada, T. Datta, and R. J. Matson, *Phys. Rev. Lett.* **60**, 937 (1988).

⁷Z. Z. Sheng and A. M. Hermann, *Nature (London)* **332**, 55 (1988).

⁸Z. Z. Sheng and A. M. Hermann, *Nature (London)* **332**, 138 (1988).

⁹R. M. Hazen, C. T. Prewitt, R. J. Angel, N. L. Ross, L. W. Finger, C. G. Hadjicacos, D. R. Veblen, P. J. Heaney, P. H. Hor, R. L. Meng, Y. Y. Sun, Y. Q. Wang, Y. Y. Xue, Z. J. Huang, L. Gao, J. Bechtold, and C. W. Chu, *Phys. Rev. Lett.* **60**, 1174 (1988).

¹⁰M. A. Subramanian, C. C. Torardi, J. C. Calabrese, J. Gopalakrishnan, K. J. Morrissey, T. R. Askew, R. B. Flippen, U. Chowdhry, and A. W. Sleight, *Science* **239**, 1015 (1988).

¹¹S. A. Sunshine, T. Siegrist, L. F. Schneemeyer, D. W. Murphy, R. J. Cava, B. Batlogg, R. B. van Dover, R. M. Fleming, S. H. Glarum, S. Nakahara, R. Farrow, J. J. Krajewski, S. M. Zahurak, J. V. Waszczak, J. H. Marshall, P. Marsh, L. W. Rupp, Jr., and W. F. Peck, to be published.

¹²J. M. Tarascon *et al.*, *Phys. Rev. B.* (to be published).

¹³A. M. Hermann and Z. Z. Sheng, *Appl. Phys. Lett.* **51**, 1854 (1987).

¹⁴D. R. Veblen, P. J. Heaney, R. J. Angel, L. W. Finger, R. M. Hazen, C. T. Prewitt, N. L. Ross, C. W. Chu, P. H. Hor, and R. L. Meng, *Nature (London)* **332**, 334 (1988).

¹⁵J. Billingham, P. S. Bell, and M. H. Lewis, *Acta Crystallogr. A* **28**, 602 (1972).

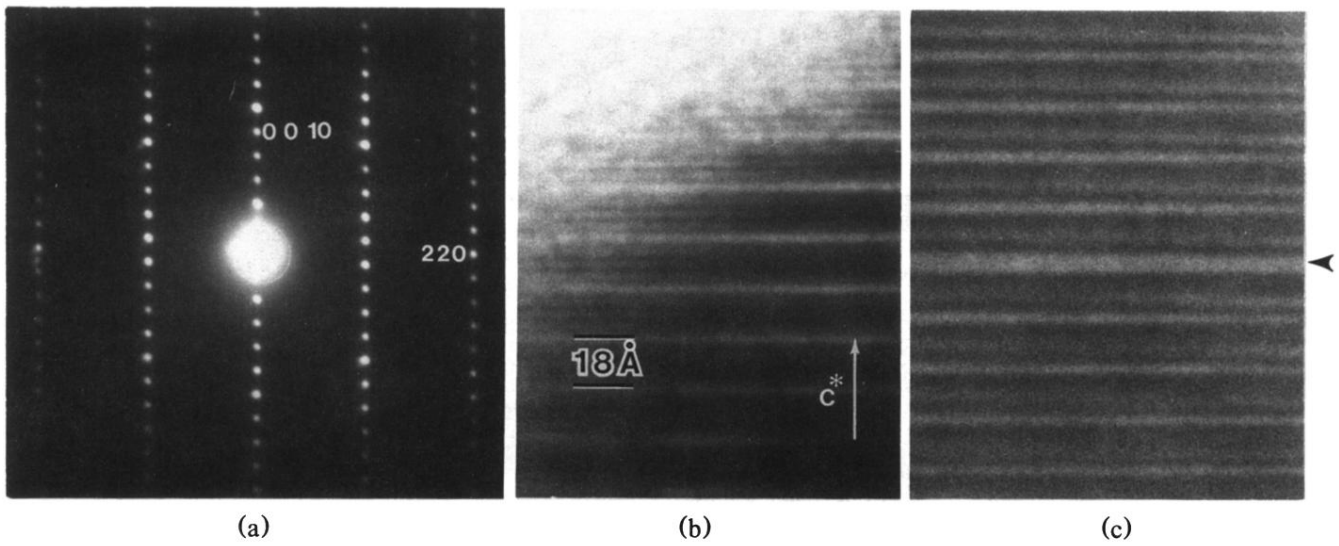


FIG. 2. (a) $[1\bar{1}0]$ Selected-area electron diffraction pattern of 2223 superconductor. (b) The corresponding lattice image reveals a prominent 18-Å layering parallel to (001), similar to that of the bismuth 2122 superconductor (Refs. 9 and 14). (c) Defects in the layering (arrow) are relatively uncommon in the 2223 phase compared to the structurally related bismuth 2122 superconductor.

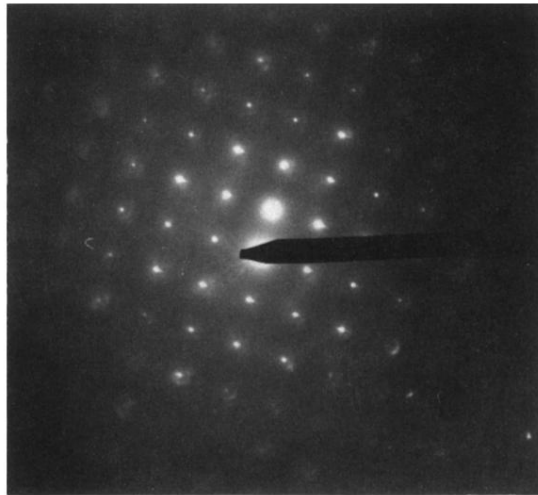


FIG. 3. Selected-area diffraction pattern of the 2223 phase reveals faint ringlike diffraction effects that surround some diffraction maxima. This pattern, which is consistent with the $[21\bar{1}]$ zone axis, may result from point-defect clusters or other short-range ordering (Ref. 15).